ELSEVIER

Effect of calcination temperature on the catalytic activity of zirconia-supported heteropoly acids

Biju M. Devassy, S.B. Halligudi [*]

Inorganic Chemistry and Catalysis Division, National Chemical Laboratory, Pune 411 008, India

Abstract

Zirconia-supported silicotungstic acid (15% STA) catalyst with different calcination temperatures (600–850 °C) was prepared by suspending zirconium oxyhydroxide in methanol solution of STA followed by drying and calcination. These catalysts were characterized by XRD, FTIR pyridine adsorption and DRUV–vis spectroscopy. The catalysts showed both Brønsted as well as Lewis acidity and 15% STA on zirconia calcined at 750 °C (15 SZ-750) had the highest Brønsted acidity. Characterization of 15 SZ-750 catalyst by Raman spectroscopy showed the presence of zirconia-anchored mono-oxotungstate as the major tungsten species present in this catalyst. These catalysts were used in benzoylation of veratrole with benzoic anhydride and 15 SZ-750 catalyst showed the highest activity. For catalyst with support calcined at different temperatures before HPA impregnation, catalytic activity decreases as the support calcination temperature increases due to the decrease in Brønsted acidity. Comparison of the catalytic activity of 15 SZ-750 with that of zirconia-supported phosphotungstic acid (15%, calcined at 750 °C, 15 PZ-750) in benzoylation of veratrole with benzoic anhydride, acylation of anisole with acetic anhydride and in alkylation of diphenylether with 1-dodecene showed that 15 SZ-750 catalyst has higher activity and deactivation resistance due to its higher Brønsted acidity. The deactivated catalyst could be regenerated by calcination without appreciable loss in activity.
© 2006 Elsevier B.V. All rights reserved.

Keywords: Zirconia; Silicotungstic acid; Phosphotungstic acid; Acylation; Alkylation; Veratrole; Anisole; Diphenylether

1. Introduction

In recent years, zirconia has attracted much attention as both a catalyst and a catalyst support because of its high thermal stability and the amphoteric character of its surface hydroxyl groups [1,2]. Zirconia modified with anions like sulfate and tungstate act as strong solid acid catalysts [3,4].

Heteropoly acids (HPAs) are [5–8] polyoxometallates made up of heteropoly anions having metal–oxygen octahedra as the basic structural unit. The Keggin type HPAs is the most important in catalysis because of their simple synthesis procedure and relatively high thermal stability. These are strong Brønsted acid catalysts and their strength of acidity is higher than that of conventional solid acids like zeolites and mixed oxides [6]. Acidic or neutral solids, which interact weakly with HPAs such as silica, active carbon and acidic ion-exchange resin, have been reported to be suitable as HPA supports [9,10]. Recently, zirconia-supported heteropoly acids attracted much attention as strong solid acid catalysts [11–14].

The present study deals with the effect of calcination temperature of the catalyst and support (before HPA impregnation) on the catalytic activity of zirconia-supported silicotungstic acid in benzoylation of veratrole with benzoic anhydride. The activity of the most active catalyst 15 SZ-750 was compared with that of 15 PZ-750 in benzoylation of veratrole with benzoic anhydride, acylation of anisole with acetic anhydride and alkylation of diphenylether with 1-dodecene.

2. Experimental

2.1. Materials

Zirconyl chloride (ZrOCl$_2$·8H$_2$O) and ammonia (25%) were obtained from S.D. Fine Chemicals Ltd., Mumbai.

---
[*] Corresponding author.
E-mail address: sb.halligudi@ncl.res.in (S.B. Halligudi).

Veratrole (98%), 12-STA ($H_4SiW_{12}O_{40} \cdot nH_2O$), 12-PTA ($H_3PW_{12}O_{40} \cdot nH_2O$) and methanol were purchased from Aldrich. Benzoic anhydride (98%) was obtained from E. Merck India Ltd., Mumbai. All the chemicals were used as received without further purification.

2.2. Catalyst preparation

The catalysts were prepared by suspending dried zirconium oxyhydroxide powder in a methanol solution of STA (4 ml methanol/g of support). The support, zirconium oxyhydroxide was prepared by hydrolysis of zirconyl chloride solution by the addition of aqueous NH_3. The precipitate formed was filtered, washed with water until free from chloride ions and dried at 120 °C for 12 h, powdered well and dried for another 12 h. The suspension mixture (STA loading, 15%) was stirred in a rotary evaporator for 8–10 h and excess of methanol was removed at ca. 50 °C under vacuum. Previous studies showed that 15% HPA loading has the better catalytic activity [12–14]. The resulting solid materials were dried at 120 °C for 24 h, ground well and calcined in air for 4 h (heating/cooling rate, 5 °C min^{-1}). For comparison, catalysts with 15% PTA on zirconia (calcined at 750 °C, 15 PZ-750) was also prepared. The catalysts with 15% STA on ZrO_2 calcined at different temperatures are represented by 15 SZ-T, where S represents STA, Z represents zirconia and T denotes calcination temperature in °C.

In order to study the effect of support calcination temperature on the catalytic activity, zirconium oxyhydroxide calcined at different temperatures used as the support and after HPA impregnation, these materials were calcined at 750 °C.

3. Results and discussion

3.1. Characterization of the catalysts

3.1.1. X-ray diffraction

The bulk structure of pure ZrO_2 and of supported HPA catalysts were determined by powder X-ray diffraction (Fig. 1A). The support shows amorphous behavior below 350 °C and crystallizes to a mixture of monoclinic and tetragonal phases and the intensity of monoclinic phase increases with the calcination temperature. Pure zirconia calcined at 750 °C is mainly monoclinic with only a small amount of the tetragonal phase.

As shown in Fig. 1B, 15% catalyst was amorphous when it was calcined below 450 °C and as the calcination temperature increases, zirconia crystallizes progressively to tetragonal phase and at 750 °C, the catalyst exists mainly in tetragonal phase, and above 750 °C, formation of monoclinic phase of zirconia was observed. The effectiveness of the surface species to stabilize ZrO_2 in tetragonal phase may lose at high temperatures because they diffuse into the bulk, decompose and desorbs, or "dewet" and agglomerate to form poorly interacting clusters as a separate phase [15]. It could also be seen that for 15% catalyst, up to 750 °C calcination, no diffraction lines attributed to the polyacid or its decomposition products were observed, indicating that STA is highly dispersed on the support. When calcination temperature exceeds 750 °C, new diffraction lines appear in the region of 23–25°, characteristic of WO_3 [16].

The XRD patterns of the catalysts with support calcined at different temperatures prior to HPA impregnation shows that catalyst is increasingly monoclinic as the support calcination temperature increases (Fig. 1C). This is because the calcination
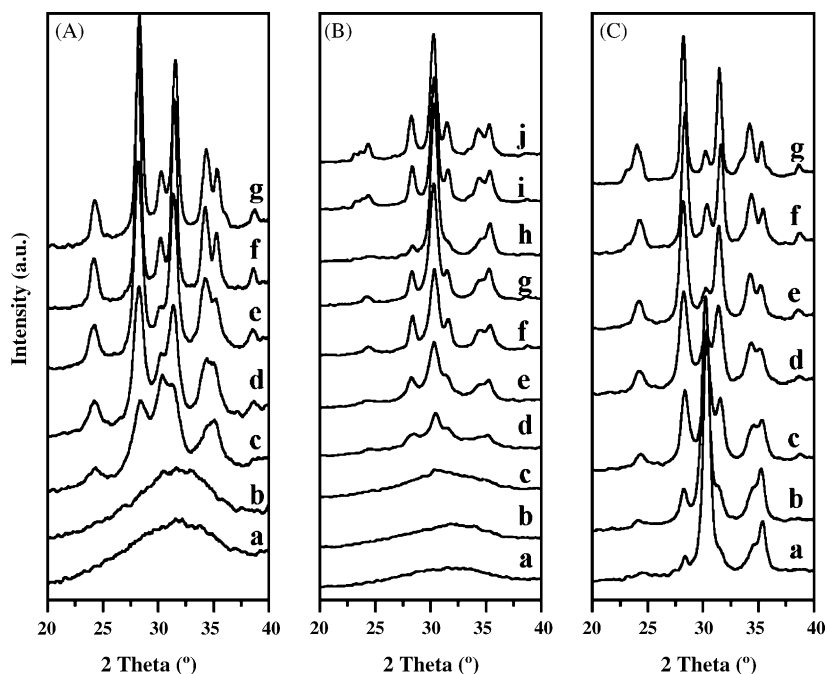

Fig. 1. XRD patterns of: (A) ZrO_2 calcined at different temperatures—(a) 120 °C, (b) 250 °C, (c) 350 °C, (d) 450 °C, (e) 550 °C, (f) 650 °C and (g) 750 °C; (B) 15 SZ calcined at different temperatures—(a) 120 °C, (b) 250 °C, (c) 350 °C, (d) 450 °C, (e) 550 °C, (f) 650 °C and (g) 750 °C; (C) catalysts with support calcined at different temperatures—(a) 120 °C, (b) 250 °C, (c) 350 °C, (d) 450 °C, (e) 550 °C, (f) 650 °C and (g) 750 °C.

of the support at high temperature changes its crystalline nature and loading of HPA on such calcined support does not have an influence on the XRD of the finally calcined material.

3.1.2. Raman spectroscopy and ^{31}P MAS NMR spectroscopy

Raman spectra of pure STA, PTA and the most active catalysts 15 SZ-750 and 15 PZ-750 are shown in Fig. 2. The strong support Raman bands below $700\,cm^{-1}$ interfere with the diagnostic Raman bands of tungstate species, while the range above $700\,cm^{-1}$ is free from characteristic bands of ZrO_2 and hence relevant to the structure determination of tungsten species. Pure STA shows a sharp band at $998\,cm^{-1}$ with a distinct shoulder at $974\,cm^{-1}$ attributed to $\nu_{(W=O)}$ symmetric and asymmetric stretching modes, respectively. In addition, another broadband observed at $893\,cm^{-1}$ is assigned to the $\nu_{(W-O-W)}$ asymmetric stretching mode [17,18]. Pure PTA shows similar type of Raman spectrum as that of pure STA. The catalysts 15 SZ-750 showed bands at 992 and $825\,cm^{-1}$ characteristic of $\nu_{(W=O)}$ and $\nu_{(W-O-Zr)}$ [19] vibrations, respectively. In addition to the bands at 825 and $992\,cm^{-1}$, the catalyst 15 SZ-750 shows an additional band at $910\,cm^{-1}$ due to $\nu_{(W-O-W)}$ stretching mode [4]. However, the relative intensity of this band is very small in comparison with other bands indicating the formation of small amount of polyoxotungstate species [4,20]. The catalyst 15 PZ-750 shows bands at 988 and $822\,cm^{-1}$ due to $\nu_{(W=O)}$ and $\nu_{(W-O-Zr)}$ vibrations, respectively. Thus, Raman spectra show the presence of zirconia-anchored hydrated mono-oxotungstate as the major tungsten species present in 15 SZ-750 and 15 PZ-750 catalysts.

The ^{31}P MAS NMR spectrum and ^{31}P CP/MAS NMR spectrum of the catalyst 15 PZ-750 is shown in Fig. 3. The NMR spectrum shows signals above and below $-20\,ppm$. The CP/MAS NMR spectrum indicates the attenuation of the signal above $-20\,ppm$ and hence this signal is attributed to P—OH group associated with phosphotungstate, which is in interaction with zirconia [14], while the signal below $-20\,ppm$ is
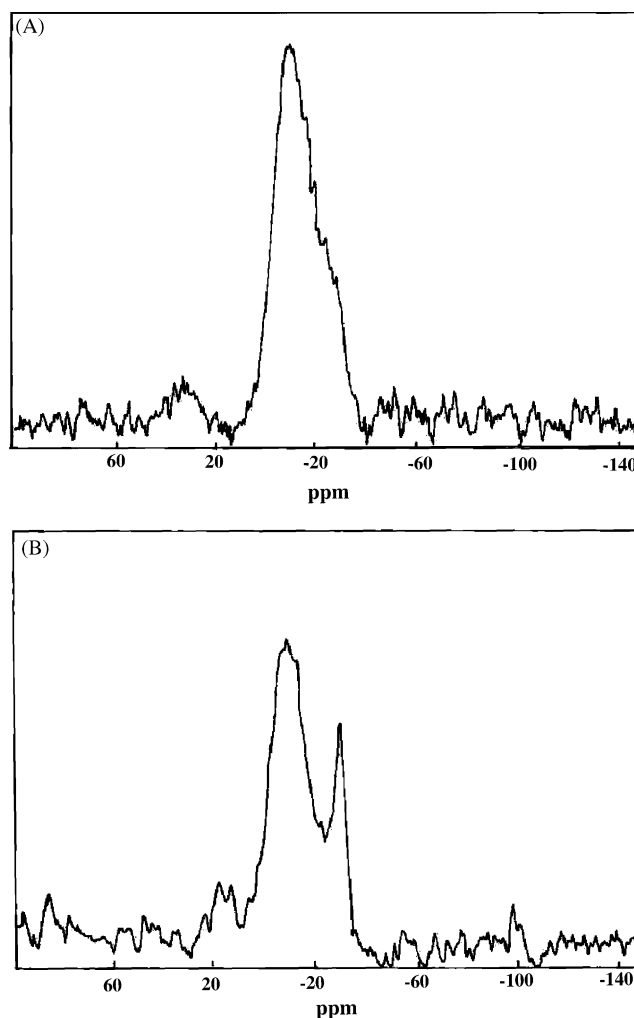

Fig. 3. ^{31}P MAS NMR spectrum (A) and ^{31}P CP/MAS NMR spectrum (B) of the catalyst 15 PZ-750.

attributed to phosphorous oxide resulting from the decomposition of phosphotungstic acid [11]. From the elemental analysis by inductively coupled plasma-optical emission spectroscopy (ICP-OES), the composition of the catalyst 15 PZ-750 is found to be $Zr = 62.22\,wt.\%$, $W = 10.13\,wt.\%$, $P = 0.15\,wt.\%$, which indicates that the P:W atomic ratio is $\sim$1:12. This result indicates that the phosphorous oxide formed by the decomposition of phosphotungstic acid was not lost by sublimation during calcination.

3.1.3. TPD of NH_3

Ammonia adsorption–desorption technique usually enables the determination of the strength of acid sites present on the catalyst surface together with total acidity. The NH_3-TPD profiles of 15 SZ catalyst calcined at different temperatures are shown in Fig. 4 and the amount of NH_3 desorbed nm^{-2} are presented in Table 1. All samples show a broad TPD profile revealing that the surface acid strength is widely distributed. For 15 SZ catalysts calcined at different temperatures, the amount of desorbed ammonia increases with calcination temperature and reaches maximum at $750\,°C$ (Table 1).
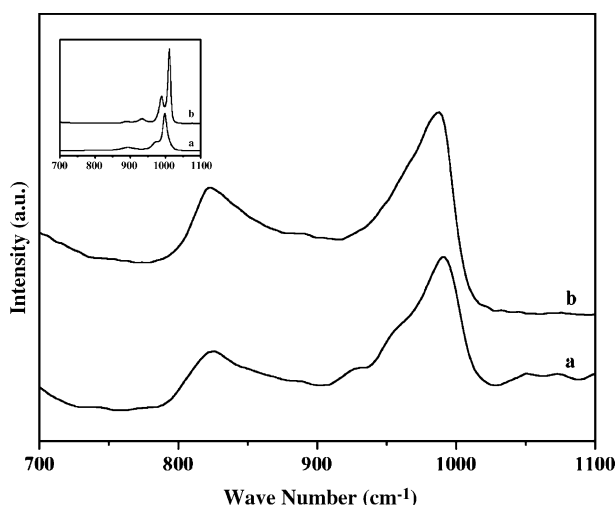

Fig. 2. Raman spectra of the catalysts: (a) 15 SZ-750 and (b) 15 PZ-750. Inset: (a) STA and (b) PTA.
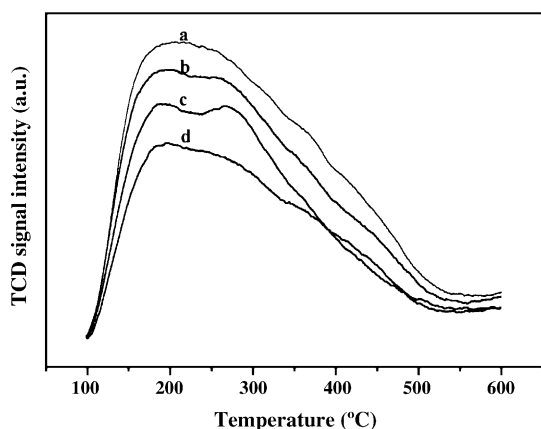
Fig. 4. NH$_3$-TPD profiles 15 SZ calcined at different temperatures: (a) 650 °C, (b) 700 °C, (c) 750 °C and (d) 800 °C.

Table 1
Acidity of 15 SZ catalyst calcined at different temperatures obtained from NH$_3$-TPD

Catalyst	Acidity (NH$_3$ nm^{-2})
Z-750	n.e.
15 SZ-600	n.e.
15 SZ-650	1.93
15 SZ-700	2.43
15 SZ-750	2.81
15 SZ-800	2.61
15 PZ-750	3.29

3.1.4. FTIR pyridine adsorption

The FTIR pyridine adsorption spectra of 15 SZ catalyst calcined at different temperatures are shown in Fig. 5A. The spectra of 15 SZ-750 catalyst shows sharp pyridine absorption bands at 1604, 1485, 1444, 1636 and 1534 cm^{-1}. Pyridine molecules bonded to Lewis acid sites absorbed at 1604 and 1444 cm^{-1}, while those responsible for Brønsted acid sites (pyridinium ion) shows absorbance at 1534 and at 1636 cm^{-1} [21]. The band at
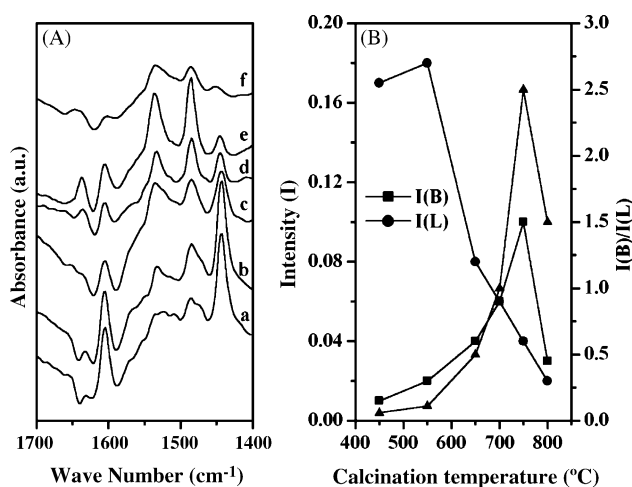

Fig. 5. (A) FTIR pyridine absorption spectra of 15 SZ-750 catalyst calcined at different temperatures: (a) 450 °C, (b) 550 °C, (c) 650 °C, (d) 700 °C, (e) 750 °C and (f) 800 °C after in situ activation at 300 °C and (B) change in B, L and B/L ratio with calcination temperature.
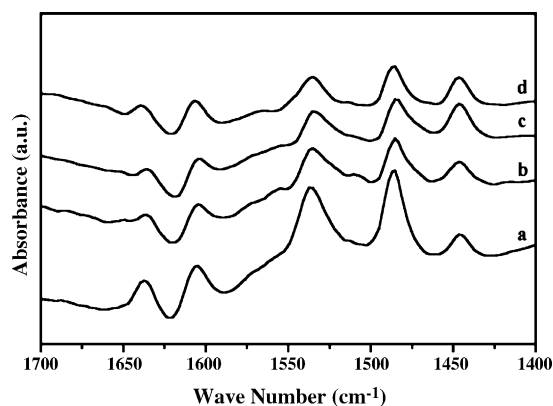

Fig. 6. FTIR pyridine adsorption spectra of catalysts with support calcined at different temperatures: (a) 120 °C, (b) 350 °C, (c) 450 °C and (d) 650 °C.

Table 2
Pyridine adsorption data for the catalysts with support calcined at different temperatures

Support calcinations temperature (°C)	I(B)	I(L)	I(B)/I(L)
120	0.1	0.04	2.5
350	0.06	0.04	1.5
450	0.06	0.05	1.2
650	0.05	0.5	1

1485 cm^{-1} is a combined band originating from pyridine bonded to both Brønsted and Lewis acid sites.

The intensity of Brønsted (B) and Lewis (L) acid sites, obtained from the absorbance at 1534 and at 1444 cm^{-1} [22], and the corresponding B/L ratio calculated are shown in Fig. 5B. At low calcination temperature (450 °C), the catalyst 15 SZ shows mainly Lewis acidity and Brønsted acidity increased with the calcination temperature up to 750 °C.

For catalysts with support calcined at different temperatures prior to HPA impregnation, Brønsted acidity decreases without appreciable change in Lewis acidity and hence the Brønsted acidic character (B/L ratio) decreases with an increase in support calcination temperature (Fig. 6 and Table 2).

The FTIR pyridine adsorption spectra of the catalysts 15 SZ-750 and 15 PZ-750 at different activation temperatures are shown in Fig. 7. The corresponding IR absorbance intensities of Brønsted and Lewis acid sites and B/L ratio at different activation temperatures are given in Table 3. The results indicate that

Table 3
Pyridine adsorption data for the catalysts 15 SZ-750 and 15 PZ-750 at different activation temperatures[a]

Activation temperature (°C)	B acidity I(B)	L acidity I(L)	B/L ratio I(B)/I(L)
100	0.19(0.15)	0.14(0.17)	1.36(0.88)
200	0.16(0.16)	0.09(0.12)	1.78(1.33)
300	0.10(0.09)	0.04(0.06)	2.50(1.5)
400	0.05(0.08)	0(0.03)	ne[b](2.67)

[a] For the catalyst 15 PZ-750, B, L and B/L values are indicated in parentheses.
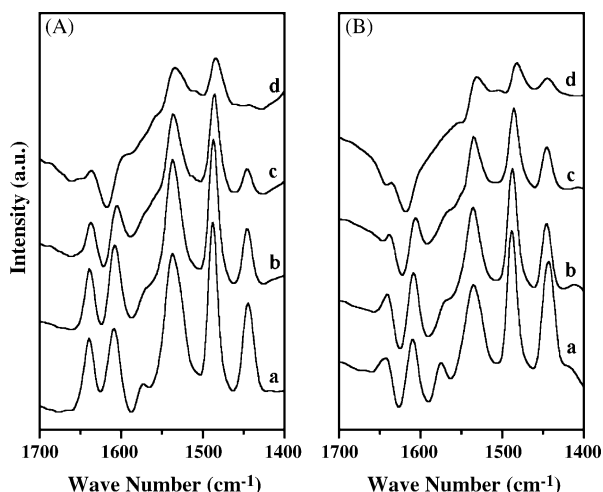[b] Not evaluated.

Fig. 7. FTIR pyridine adsorption spectra of: (A) 15 SZ-750 and (B) 15 PZ-750 catalysts at different activation temperatures—(a) 100 °C, (b) 200 °C, (c) 300 °C and (d) 400 °C.
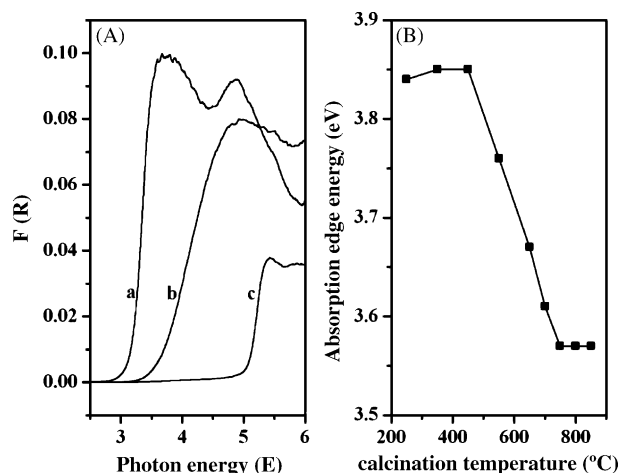

Fig. 8. (A) DRUV–vis absorption spectra of: (a) pure STA, (b) 15 SZ-750 and (c) Z-750 and (B) change in absorption edge energies of 15 SZ calcined at different temperatures.

an increase of activation temperature results in a decrease in both Brønsted and Lewis acidity but an overall increase in Brønsted character (B/L ratio) of the catalyst. These results clearly show that the strength of Brønsted acid sites is higher than that of Lewis acid sites. Moreover, the catalyst 15 SZ-750 shows higher Brønsted acidity, while 15 PZ-750 shows higher Lewis acidity at all activation temperatures.

It has been reported that pure STA shows mainly Brønsted type acidity. The support zirconium oxyhydroxide is shown to be amphoteric in character. The interaction of zirconium oxyhydroxide with HPA neutralizes the Brønsted acid sites of HPA and from $(Zr(OH_2)_n{}^+)(H_{3-n}W_{12}O_{40})$ like species [11]. The 15 SZ catalyst calcined at lower temperature is mainly Lewis acidic in nature and Brønsted acidity increases with calcination temperature. The higher Lewis acidity at lower calcination temperature shows that the Lewis acidity mainly originates from the support itself. At higher calcination temperature, dehydration/dehydroxylation occurs and the interaction HPA with the support increases and STA anchored to zirconia through Zr−O−W bond, and during this process, new Brønsted acid sites are generated. Formation such Brønsted acid sites are also observed in zirconia-supported isopolytungstate catalysts.

3.1.5. Diffuse-reflectance UV–vis spectroscopy

Diffuse reflectance UV–vis spectra of pure STA, 15 SZ-750 and Z-750 are shown in Fig. 8A. For pure STA, bands are observed in the range of 3–5.5 eV arising from low-energy O^{2-} to W^{6+} charge transfer. The energy of an electronic transition can be characterized by the position of the energy of maximum absorption [23]. Since the charge transfer bands are broad for zirconia-supported STA catalysts, charge-transfer transitions are more accurately characterized by energy at the absorption edge. The fundamental optical absorption edge energy were determined with a procedure reported by Barton et al. [24] from the intercept of $[F(R)h\nu]^{1/2}$ plotted versus $h\nu$, where $F(R)$ is Kubelka-Munk function and $h\nu$ is the energy of the incident photon.

The absorption edge energies for 15 SZ catalyst calcined at different temperatures are shown in Fig. 8B. Pure STA shows absorption edge energy of 3.19 eV, while pure ZrO_2 shows absorption edge energy of 5.04 eV. After supporting STA on zirconium oxyhydroxide (15%) followed by drying at 250 °C, the edge energy is increased to 3.84 eV. The increase in the edge energy compared to bulk STA is due to the effect of the support, which spreads silicotungstate and thus decreases the interaction between the polyanions [25]. There is no appreciable change in edge energy for the catalyst 15 SZ up to a calcination temperature of 450 °C. Further increase in calcination temperature decreases the edge energy up 750 °C. Thus, the decrease in absorption edge energy with calcination temperature up to 750 °C could be explained based on the interaction between polyanion. As the calcination temperature increases, silicotungstate undergoes agglomeration and these results in an increase in interaction between polyanion, which could be considered as equivalent to the formation of a larger polyanion resulting in decrease of absorption edge energy [25,26].

The increase in Brønsted acidity with calcination temperature can be explained based on the interaction between polyanion and hence the formation of larger polyanion. Polyanion with larger size can effectively delocalize the negative charge required for the formation of Brønsted acid centers and this ultimately results in an increase in Brønsted acidity.

3.2. Catalytic activity

The benzoylation of veratrole with benzoic anhydride (BA) over supported-HPA catalysts lead to 3,4-dimethoxy benzophenone as the benzoylated product. The conversion was expressed as the percentage of BA converted into the product, the conversion of BA increased from 0.5 to 46% as the calcination temperature increased from 600 to 750 °C, and decreases further (Fig. 9A). For catalysts, where support calcined at different temperatures, conversion of BA decreases with an increase in calcination temperature (Fig. 9B). The conversion of BA was 46% for the catalyst with support calcined at 120 °C, decreased
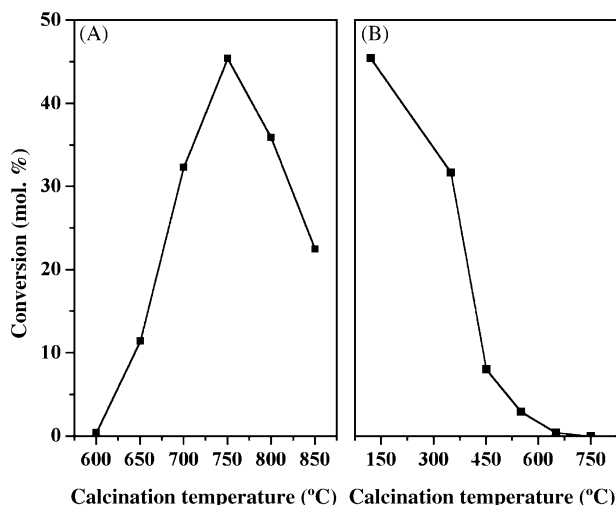
Fig. 9. Change in benzoic anhydride (BA) conversion with: (A) catalyst calcination temperature and (B) support calcination temperature (reaction conditions: total weight, 5 g; catalyst weight, 0.15 g; veratrole/BA (molar ratio) = 5; time, 1 h).
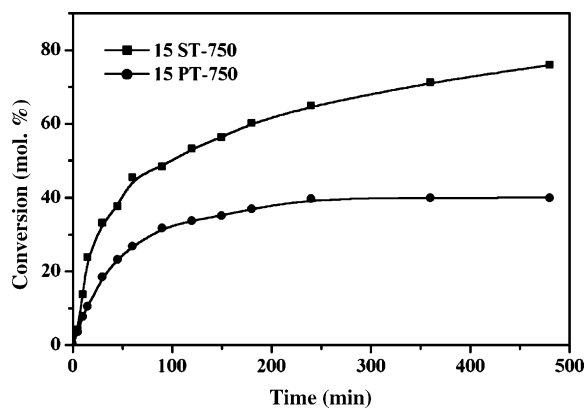

Fig. 10. Effect of time on BA conversion over (■) 15 SZ-750; (●) 15 PZ-750 catalysts (reaction conditions: temperature, 80 °C; total weight, 5 g; veratrole/BA (molar ratio) = 5; catalyst weight, 0.15 g).

to 8% at 450 °C and further decreased to 0.5% at 650 °C. Comparison of the catalytic activity of 15 SZ-750 catalyst with that of silica-supported silicotungstic acid catalyst showed that the latter catalyst leaches into the reaction medium during reaction and catalyze the reaction homogeneously [14].

Acidity measurements of the catalysts by FTIR pyridine adsorption show that the catalyst 15 SZ-750 possess the highest Brønsted acidity and Brønsted acidity decreases with an increase in support calcination temperature which clearly indicates that benzoylation of veratrole by benzoic anhydride is catalyzed by Brønsted acid sites present in the supported-catalyst. The results show that the activity of the catalyst strongly depends on the calcination temperature of the support prior to HPA impregnation. The decrease in the conversion of BA with an increase in calcination temperature of the support could be due to the decease in surface OH groups [27]. Heteropoly anions in order to anchor to the surface of zirconia and form Zr−O−W bond (see Raman spectra); need the presence of surface hydroxyl groups. Therefore, the depletion of surface OH groups hampers the possibilities of this bond formation. Calcination results in progressive oxolation in the bulk and on the surface, the process is more pronounced in the temperature interval corresponding to the "glow exotherm", 430–450 °C as detected by DTA experiments [13,27]. Oxolation on the surface produces oxo bridges, which are relatively inert towards HPA, it just deposits on the surface during impregnation and in the absence of interaction with surface hydroxyl groups decomposes to bulk WO_3 during calcination. The formation of bulk WO_3 is not clear from XRD patterns of the catalysts with support calcined at higher temperatures and this could be due to the overlap of diffraction lines of monoclinic ZrO_2 with that of bulk WO_3 (Fig. 1C). However, the presence of bulk WO_3 in catalysts where support calcined at higher temperatures is apparent from the light yellow color of these catalysts.

The catalyst 15 SZ-750 selected to compare its activity with that of the catalyst 15 PZ-750 (Fig. 10). The catalysts 15 SZ-750 showed different reaction profile from that of 15 PZ-750 in benzoylation of veratrole with benzoic anhydride. In order to study the heterogeneity of the catalysts, reaction stopped after 15 min, the catalyst separated under hot conditions, and the hot filtrate is monitored for further reaction up to 4 h. There was no change in BA conversion with time for filtrates obtained from the catalysts 15 SZ-750 and 15 PZ-750 and this indicates that STA and PTA on zirconia act as heterogeneous catalysts.

However, it is interesting to note that both the heterogeneous catalysts, 15 SZ-750 and 15 PZ-750 showed different catalytic behavior in veratrole benzoylation. For 15 SZ-750 catalyst conversion of benzoic anhydride, BA increased continuously with time and reached 76% after 480 min while, for 15 PZ-750 catalyst a clear deactivation occurred by reaching a plateau between 240 and 480 min before giving maximum conversion. This reaction profile, particularly with 15 PZ-750 catalyst is similar to that reported for zeolites [28–30] and heteropoly acids [31–34] catalyzed acylation reactions, where the catalyst deactivation is mainly attributed to the strong adsorption of the acylated product on the catalyst surface, which blocks the accessibility of the reactants to the active sites. The kinetic profile of the reaction with 15 SZ-750 and 15 PZ-750 catalysts indicated that product inhibition is more prominent with 15 PZ-750 catalyst (Fig. 10).

Similarly, the catalysts, 15 SZ-750 and 15 PZ-750 also showed different catalytic behavior in acylation of anisole with acetic anhydride (Fig. 11). The acylation of anisole with acetic anhydride (Ac_2O) lead to *para*-methoxyacetophenone as the major acylated product (selectivity ∼96%) with small amount of *ortho*-methoxyacetophenone. For both catalysts, conversion of acetic anhydride, Ac_2O increased with time upto 45 min and reached 25% for 15 SZ-750 and 12% for 15 PZ-750 catalysts and a clear deactivation thereafter by reaching a plateau between 45 and 120 min before giving maximum conversion. The 15 SZ-750 catalyst shows higher conversion and more deactivation resistance compared to 15 PZ-750 catalyst.

Thus, 15 SZ-750 catalyst was used to study different reaction parameters like reaction temperature and anisole-to-Ac_2O molar ratio on Ac_2O conversion (Fig. 12). An increase in reaction temperature from 90 to 110 °C increases the Ac_2O conversion from 27 to 52%. Since adsorption is exothermic process, the deac-
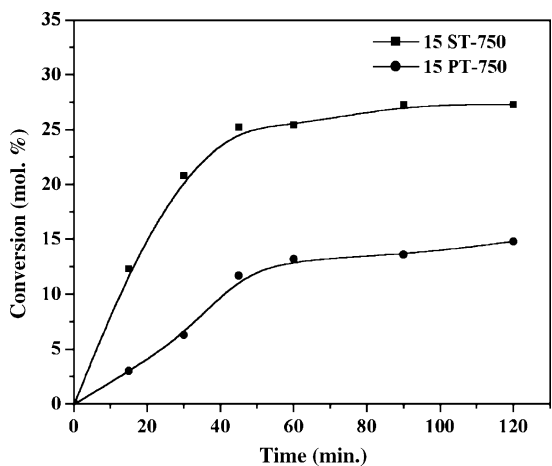
Fig. 11. Effect of time on Ac_2O conversion over (■) 15 SZ-750; (●) 15 PZ-750 catalysts (reaction conditions: temperature, 90 °C; total weight, 10 g; anisole/Ac_2O (molar ratio) = 5; catalyst weight, 0.1 g).
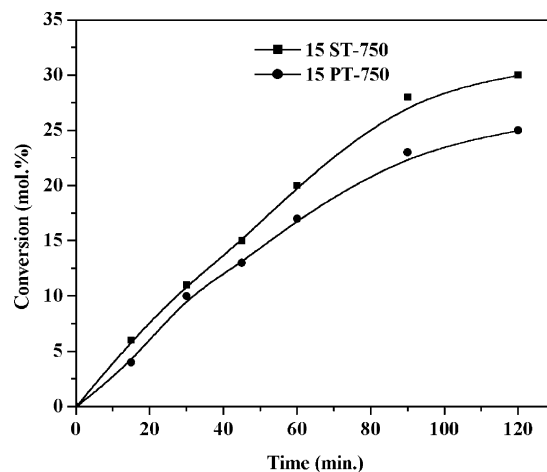

Fig. 13. Effect of time on dodecene conversion over (■) 15 SZ-750; (●) 15 PZ-750 catalysts (reaction conditions: temperature, 90 °C; total weight, 10 g; DPE/1-dodecene (molar ratio) = 10; catalyst weight, 0.3 g).

tivation of catalyst by adsorption of product on the surface of catalyst is lower at higher reaction temperature. Hence, catalyst deactivation by product inhibition is lower at high reaction temperature. The influence of anisole-to-Ac_2O molar ratio (1–10) on Ac_2O conversion was studied keeping the total weight of the reaction mixture constant. Conversion of Ac_2O increases with an increase in anisole-to-Ac_2O molar ratio. At a molar ratio of 1, the Ac_2O conversion was 13% and as the molar ratio increased to 10, conversion increased to 77%. This is probably due to the inhibiting effect of methoxyacetophenone, which can strongly adsorb on the catalyst surface. This inhibiting effect would be less significant for mixtures richer in anisole, because the excess of anisole acts as a solvent for the ketone produced, product inhibition reduced, and therefore the Ac_2O conversion is higher at higher anisole-to-Ac_2O molar ratio [28,35].

Finally, the catalysts 15 SZ-750 and 15 PZ-750 used in alkylation of diphenylether with 1-dodecene (Fig. 13) at 90 °C. In

Fig. 12. Effect of reaction conditions on Ac_2O conversion. (A) Effect of temperature (reaction conditions: total weight, 10 g; anisole/Ac_2O (molar ratio) = 5; catalyst weight, 0.1 g). (B) Effect of molar ratio (reaction conditions: temperature, 90 °C; total weight, 10 g; catalyst weight, 0.1 g).

this reaction both catalysts showed similar reaction profile, but 15 SZ-750 catalyst showed higher activity (30% dodecene conversion) than 15 PZ-750 catalyst (25% dodecene conversion). The conversion of dodecene was increased to 99% at 110 °C with 15 SZ-750 catalyst (reaction conditions: diphenylether-to-1-dodecene molar ratio = 10; total weight of the reaction mixture, 10 g; catalyst weight, 0.3 g; time 1 h). The alkylation of diphenylether with 1-dodecene to monododecyl diphenylether is important as it used as the raw materials for the production of surfactants [36].

The recyclability of the catalyst tested in alkylation of diphenylether with 1-dodecene. For recycling, the catalyst after reaction (reaction conditions: temperature, 110 °C; diphenylether-to-1-dodecene molar ratio = 10; total weight of the reaction mixture, 10 g; catalyst weight, 0.3 g; time, 1 h) was separated, washed with dichloromethane, dried at 120 °C for 4 h and reused with fresh reaction mixture. After first use, the catalyst retains only 30% of initial conversion. The lower activity of the separated catalyst could be due the blockage of active sites of the catalyst by heavy aromatics and oligomerised dodecene [12]. However, the catalytic activity is increased to 95% of initial activity after regeneration of the catalyst by calcination at 500 °C for 4 h.

In order to explain the difference in the catalytic behavior, the catalysts 15 SZ-750 and 15 PZ-750 were characterized by different methods. The surface area (55 $m^2 g^{-1}$ for 15 SZ-750 and 53 $m^2 g^{-1}$ for 15 PZ-750), XRD and Raman spectra of the catalysts were found to be similar for both the catalysts. Absorption edge energy of 15 PZ-750 catalyst (3.7 eV) was slightly higher than that of 15 SZ-750 catalyst (3.57 eV). NH_3-TPD showed that 15 PZ-750 catalyst has slightly higher acidity (3.29 NH_3 nm^{-2}) than that of 15 SZ-750 catalyst (2.81 NH_3 nm^{-2}). However, FTIR pyridine adsorption studies revealed that the Lewis acidity of 15 PZ-750 catalyst was higher than that of 15 SZ-750 catalyst (Table 2). Bachiller-Baeza and Anderson have reported that the catalyst with higher Lewis acidity is more susceptible for deactivation by product inhibition [37]. Thus, the higher conversion and greater deactivation resistance of 15 SZ-750 catalyst in ben-
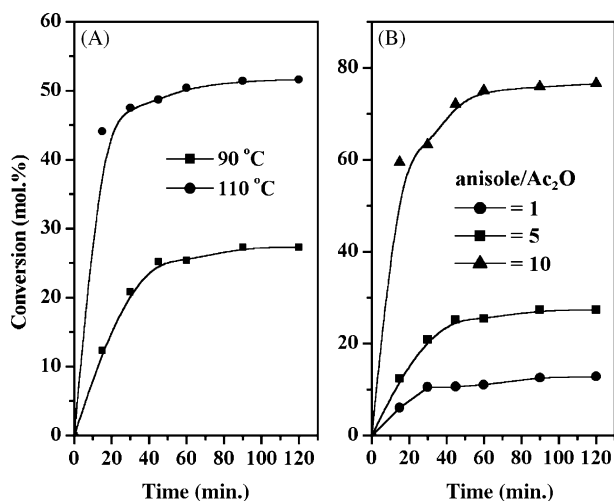
zoylation of veratrole and acylation of anisole could be due to the presence of higher amount of strong Brønsted acid sites. Similarly, the higher activity of 15 SZ-750 catalyst in diphenylether alkylation in comparison with 15 PZ-750 also could be explained based on its higher Brønsted acidity.

4. Conclusions

Zirconia-supported silicotungstic acid (15% STA) catalyst calcined at 600–850 °C were used in benzoylation of veratrole with benzoic anhydride and the catalyst calcined at 750 °C (15 SZ-750) showed the highest activity. For catalysts with support calcined at different temperatures, catalytic activity decreases with increase in support calcination temperature. Comparison of the catalytic activity of 15 SZ-750 with 15% phosphotungstic acid supported on zirconia calcined at 750 °C (15 PZ-750) in acylation and alkylation of aromatics showed that 15 SZ-750 catalyst is more active and resistant to deactivation by product inhibition in acylation reactions. The higher activity and higher deactivation resistance of 15 SZ-750 catalyst compared to 15 PZ-750 catalyst is due to its higher Brønsted acidity.

Acknowledgements

References

[1] K. Tanabe, T. Yamaguchi, Catal. Today 20 (1994) 185.
[2] G.K. Chuah, Catal. Today 49 (1999) 131.
[3] G.D. Yadav, J.J. Nair, Micropor. Mesopor. Mater. 33 (1999) 1.
[4] S. Kuba, P. Lukinskas, R.K. Grasselli, B.C. Gates, H. Knözinger, J. Catal. 216 (2003) 353 (and reference there in).
[5] M.T. Pope, Heteropoly and Isopoly Oxometalates, Springer–Verlag, Berlin, 1983.
[6] T. Okuhara, N. Mizuno, M. Misono, Adv. Catal. 41 (1996) 113.
[7] C.L. Hill (Ed.), Chem. Rev. 98 (1998) 1.
[8] N. Essayem, Y.Y. Tong, H. Jobic, J.C. Védrine, Appl. Catal. A. 194/195 (2000) 109.
[9] Y. Wu, X. Ye, X. Yang, X. Wang, W. Chu, Y. Hu, Ind. Eng. Chem. Res. 35 (1996) 2546.
[10] F. Marme, G. Coudurier, J.C. Védrine, Micropor. Mesopor. Mater. 22 (1998) 151.
[11] E. Lopez-Salinas, J.G. Hermandez-Cortez, I. Schifter, E. Torres-Garcia, J. Navarrete, A. Gutierrez-Carrillo, T. Lopez, P.P. Lottici, D. Bersani, Appl. Catal. A 193 (2000) 215.
[12] B.M. Devassy, S.B. Halligudi, S.G. Hegde, A.B. Halgeri, F. Lefebvre, Chem. Commun. (2002) 1074.
[13] B.M. Devassy, F. Lefebvre, S.B. Halligudi, J. Catal. 231 (2005) 1.
[14] B.M. Devassy, S.B. Halligudi, J. Catal. 236 (2005) 313.
[15] D.G. Barton, S.L. Soled, G.D. Meitzner, G.A. Fuentes, E. Iglesia, J. Catal. 181 (1999) 57.
[16] JCPDS, International Center for Diffraction Data, 1990, Card 43-1035.
[17] C. Rocchiccioli-Deltcheff, M. Fournier, R. Franck, R. Thouvenot, Inorg. Chem. 22 (1983) 207.
[18] C.M. Teague, X. Li, M.E. Biggin, L. Lee, J. Kim, A.A. Gewirth, J. Phys. Chem. B 108 (2004) 1974.
[19] S. Loridant, C. Feche, N. Essayem, F. Figueras, J. Phys. Chem. B 109 (2005) 5631.
[20] M. Scheithauer, R.K. Grasselli, H. Knözinger, Langmuir 14 (1998) 3019.
[21] G. Busca, Catal. Today 41 (1998) 191.
[22] B.H. Davis, R.A. Keogh, S. Alerasool, D.J. Zalewski, D.E. Day, P.K. Doolin, J. Catal. 183 (1999) 45.
[23] A. Khodakov, J. Yang, S. Su, E. Iglesia, A.T. Bell, J. Catal. 177 (1998) 343.
[24] D.G. Barton, M. Shtein, R.D. Wilson, S.L. Soled, E. Iglesia, J. Phys. Chem. B 103 (1999) 630.
[25] M. Fournier, C. Louis, M. Che, P. Chaquin, D. Masure, J. Catal. 119 (1989) 400.
[26] D. Masure, P. Chaquin, C. Louis, M. Che, M. Fournier, J. Catal. 119 (1989) 415.
[27] C.R. Vera, J.M. Parera, J. Catal. 165 (1997) 254.
[28] D. Rohan, C. Canaff, E. Fromentin, M. Guisnet, J. Catal. 177 (1998) 296.
[29] E.G. Derouane, C.J. Dillon, D. Bethell, S.B. Derouane-Abd Hamid, J. Catal. 187 (1999) 209.
[30] E.G. Derouane, G. Crehan, C.J. Dillon, D. Bethell, H. He, S.B. Derouane-Abd Hamid, J. Catal. 194 (2000) 410.
[31] J. Kaur, K. Griffin, B. Harrison, I.V. Kozhevnikov, J. Catal. 208 (2002) 448.
[32] I.V. Kozhevnikov, Appl. Catal. A 256 (2003) 3.
[33] L.A.M. Cardoso, W.A. Gomes Jr., A.R.E. Gonzaga, L.M.G. Aguiar, H.M.C. Andrade, J. Mol. Catal. A 209 (2004) 189.
[34] B. Bachiller-Baeza, J.A. Anderson, J. Catal. 228 (2004) 225.
[35] P. Botella, A. Corma, J.M. López-Nieto, S. Valencia, R. Jacquot, J. Catal. 195 (2000) 161.
[36] D. Bob, T. Oswald, J. Can. Pet. Technol. 30 (1991) 133.
[37] B. Bachiller-Baeza, J.A. Anderson, J. Catal. 228 (2004) 225.